Electronic Supplementary Material (ESI) for Physical Chemistry Chemical Physics.

Supporting Information

A computational study on bifunctional 1T-MnS_2 with adsorption-catalysis effect for lithium-sulfur batteries

Shaorong Duan,[a] Mingyi Liu,[a] Chuanzhao cao,[a] Haitao Liu,[b,*] Meng Ye,[c,*] Wenhui Duan[d,e,f,g]

[a] *Huaneng Clean Energy Research Institute, Beijing 102209, China*
[b] *Laboratory of Computational Physics, Institute of Applied Physics and Computational Mathematics, Beijing 100088, China; E-mail: liu_haitao@iapcm.ac.cn*
[c] *Graduate School of China Academy of Engineering Physics, Beijing 100193, China; E-mail: mye@gscaep.ac.cn*
[d] *State Key Laboratory of Low Dimensional Quantum Physics and Department of Physics, Tsinghua University, Beijing 100084, China*
[e] *Institute for Advanced Study, Tsinghua University, Beijing 100084, China*
[f] *Frontier Science Center for Quantum Information, Beijing 100084, China*
[g] *Collaborative Innovation Center of Quantum Matter, Beijing 100084, China*

Contents:

Number of figures: 13

Number of tables: 7

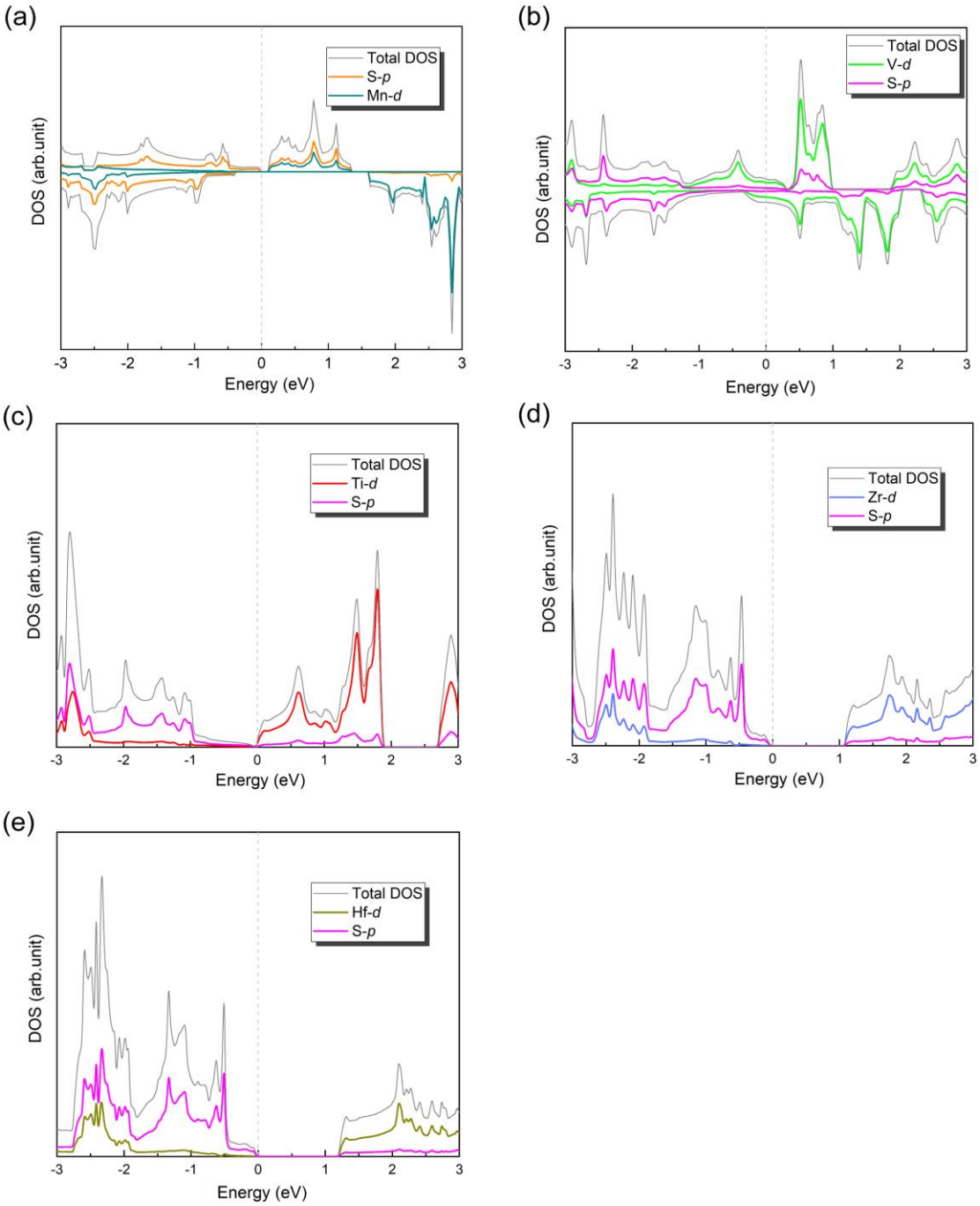

Fig. S1 Density of states of (a)1T-MnS_2, (b)1T-VS_2, (c) 1T-TiS_2, (d) 1T-ZrS_2 and (e) 1T-HfS_2. The gray dashed line represents the Fermi level. The total density of states of 1T-MS_2, *p* orbitals of sulfur atoms and *d* orbitals of metal atoms in 1T-MS_2 are represented by three different color curves. Our electronic structure calculations show 1T-TiS_2 and 1T-VS_2 are a semimetal and a metal respectively, and 1T-MnS_2, 1T-ZrS_2 and 1T-HfS_2 are semiconductors.

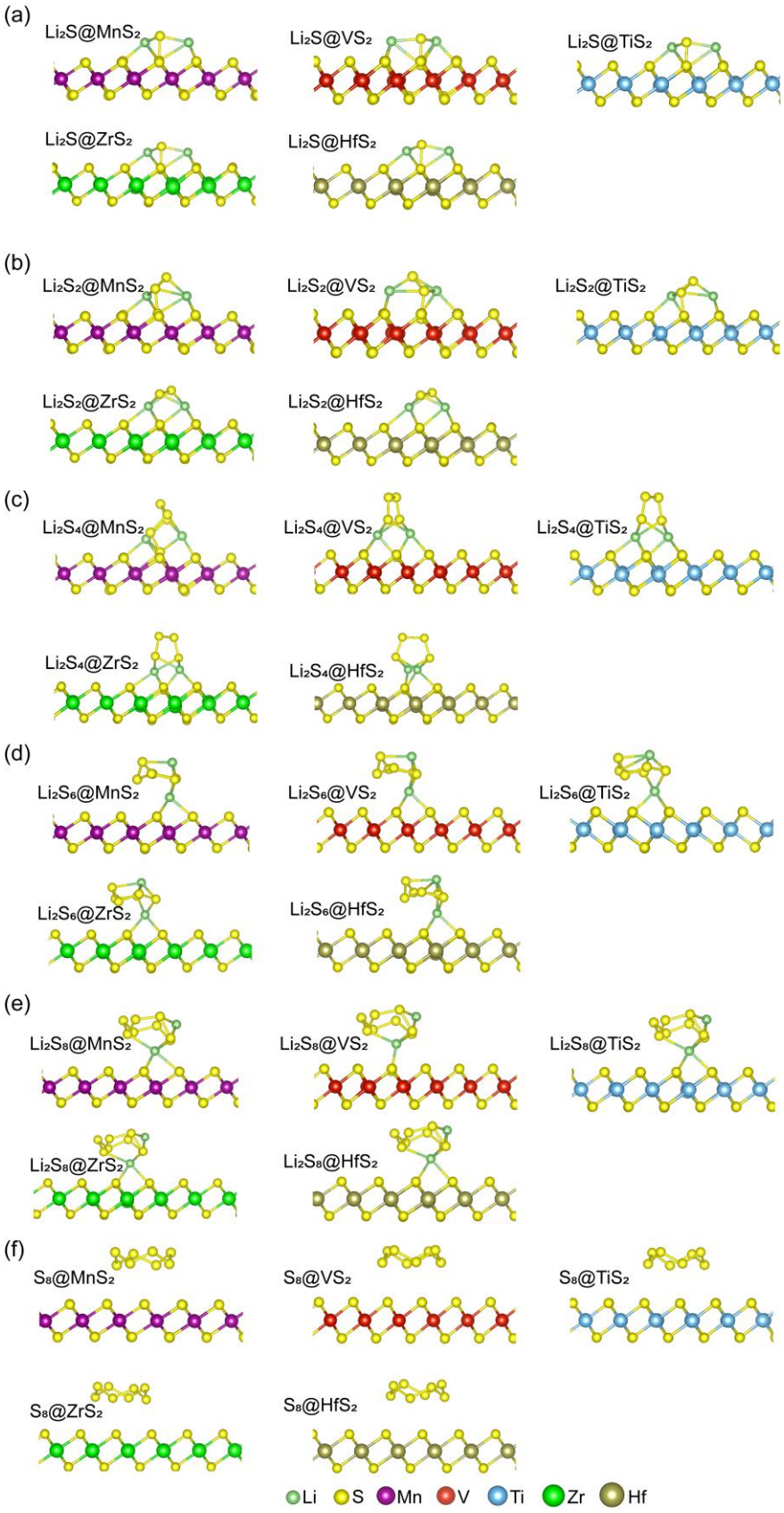

Fig. S2 The adsorption configurations of all Li_2S_n (n=1,2,4,6,8) and S_8 molecules on the surface of five 1T-MS_2.

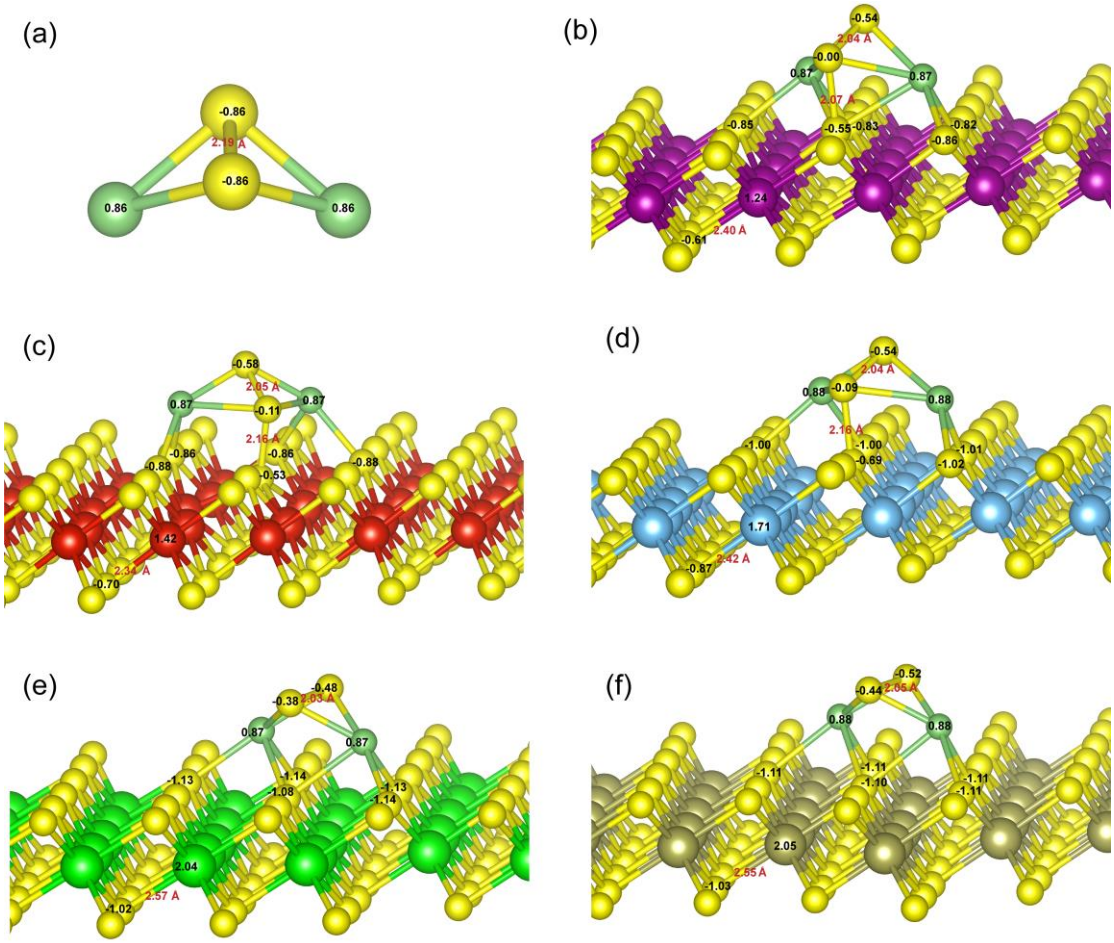

Fig. S3 The Bader charge transfer distribution of the adsorption configuration for Li_2S_2 on five 1T-MS_2 surfaces. The black number represents the change in the charge of the nearest atom, the negative number represents the charge gained by the atom, and the positive number represents the charge lost by the atom, and the red number is the bond length of S-$S_{surface}$ bond. (a) Isolated Li_2S_2 molecule in vacuum, (b) Li_2S_2@1T-MnS_2, (c) Li_2S_2@1T-VS_2, (d) Li_2S_2@1T-TiS_2, (e) Li_2S_2@1T-ZrS_2 and (f) Li_2S_2@1T-HfS_2.The Li, S, Mn, V, Ti, Zr, and Hf atoms are marked as green, yellow, purple, red, cyan, thick green, and brown, respectively.

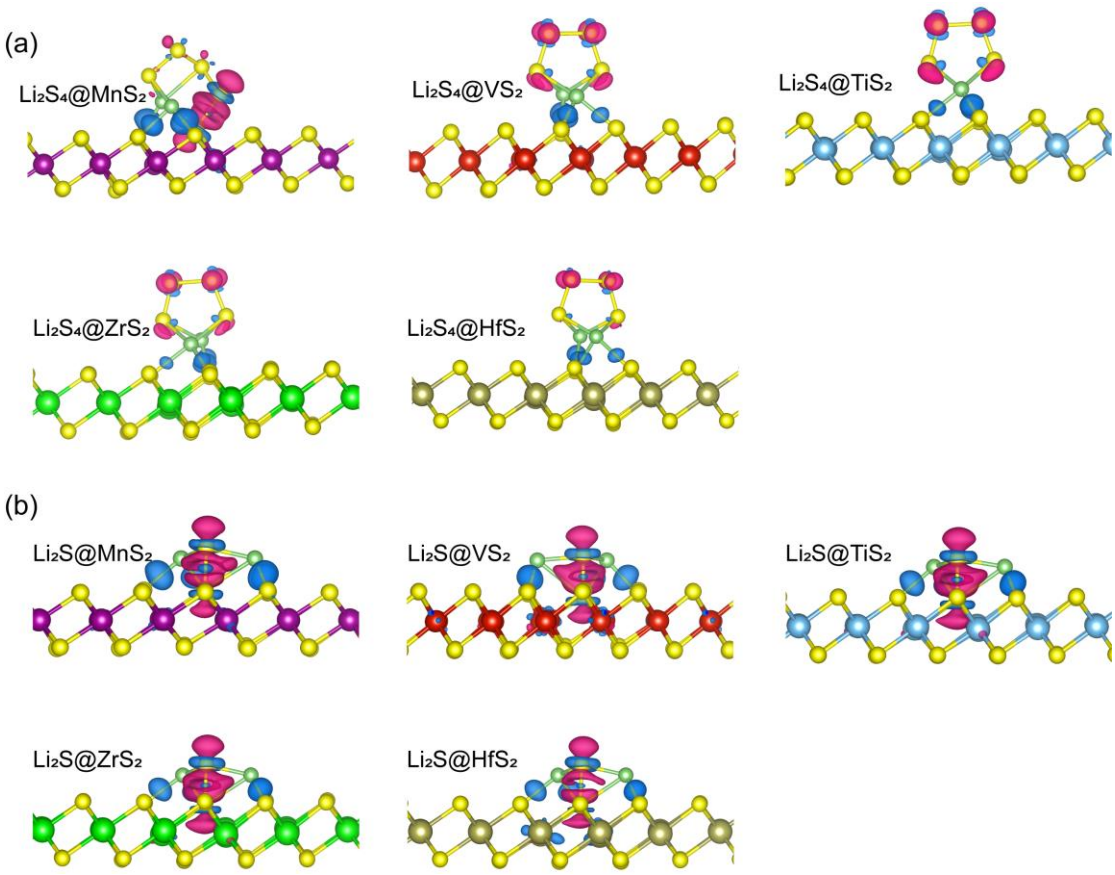

Fig. S4 The differential charge density for (a) Li_2S_4 molecule and (b) Li_2S molecule on 1T-*M*S_2 surfaces. The bule and rose red surfaces correspond to the charge accumulation and depletion regions, respectively. The isovalue is 0.0055 e•Å^{-3}. The green, yellow, purple, red, cyan, thick green and brown balls are Li, S, Mn, V, Ti, Zr and Hf atoms, respectively.

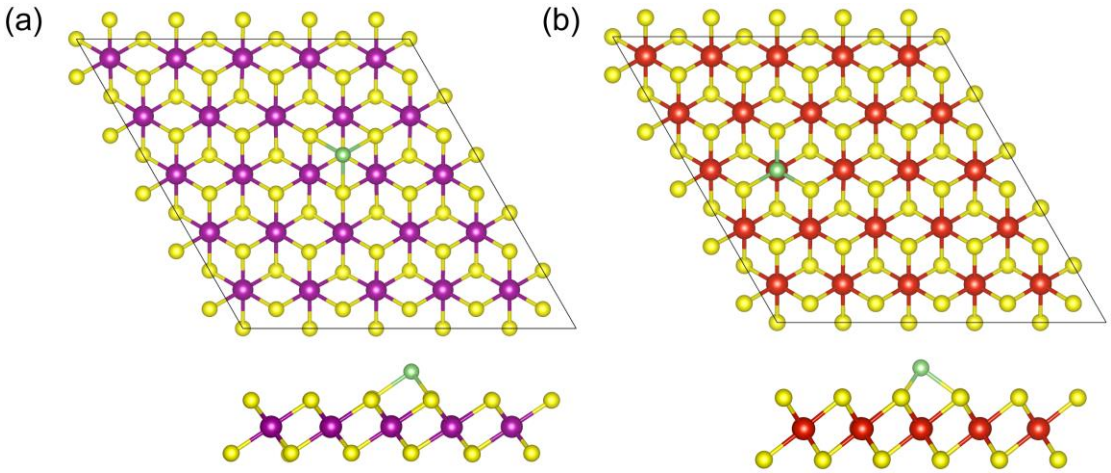

Fig. S5 The most stable adsorption configurations for Li atom on (a) 1T-MnS_2 and (b) 1T-VS_2 surfaces.

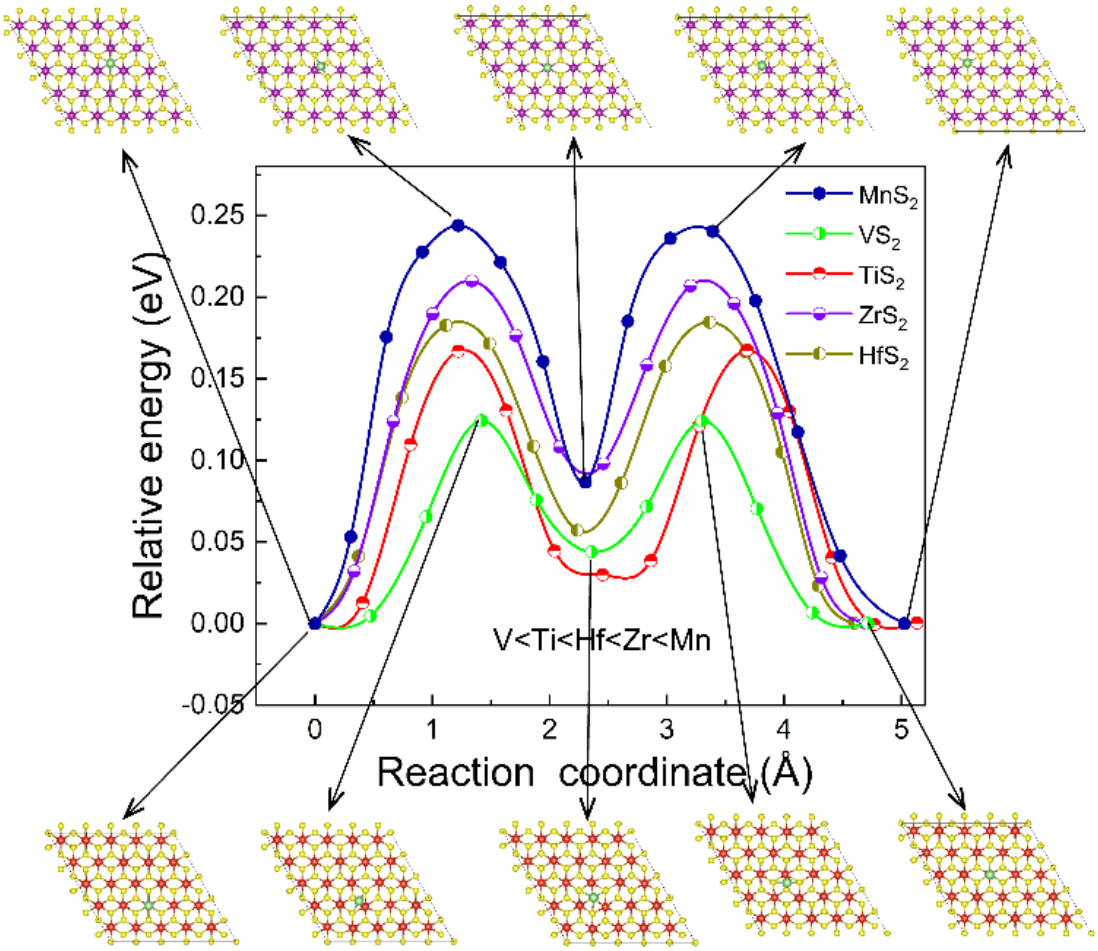

Fig. S6 The energy profile and atomic structure evolution for Li-ion diffusion on 1T-MnS_2 and 1T-VS_2 surfaces. The Li, S, Mn, and V atoms are marked as green, yellow, purple and red, respectively. The five images in the top row demonstrate the evolution of the atomic structure of Li ion diffusion on the surface of 1T-MnS_2 along C-B-C path, while the five images in the bottom row demonstrate the evolution of the atomic structure of Li ion diffusion on the surface of 1T-VS_2 along B-C-B path.

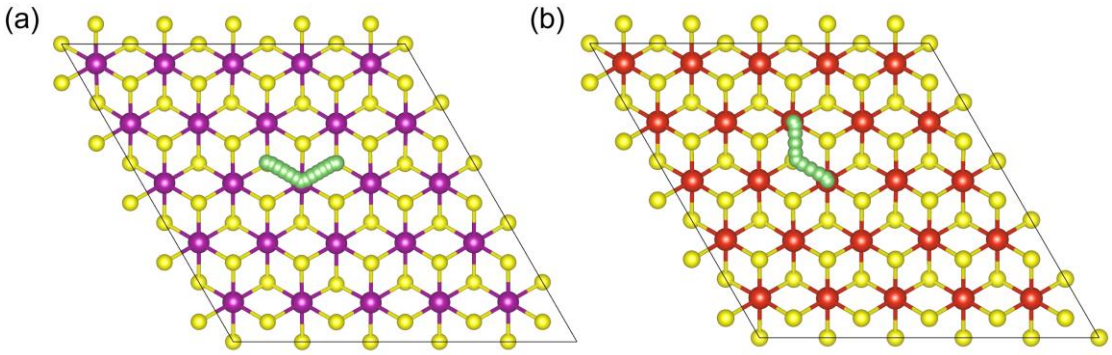

Fig. S7 The schematic diagrams for the diffusion of Li ion on (a) 1T-MnS_2 surface and (b) 1T-VS_2 surface. The Li, S, Mn, and V atoms are marked as green, yellow, purple and red, respectively.

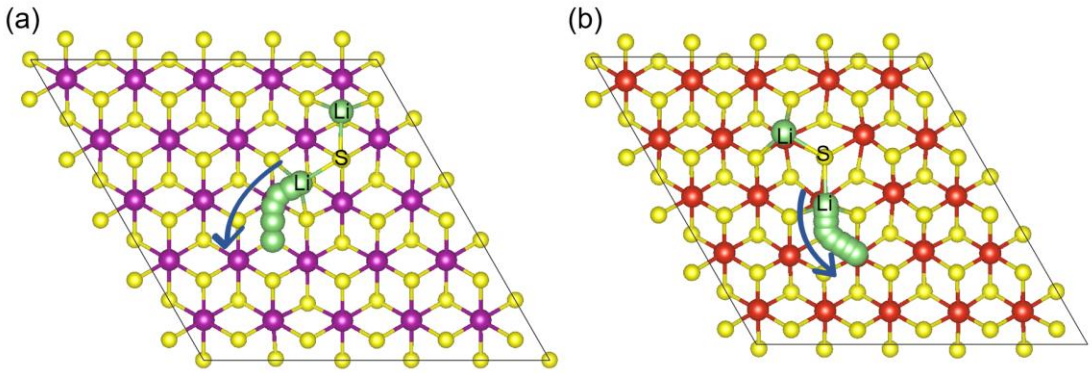

Fig. S8 The schematic diagram for the decomposition of Li_2S on (a) 1T-MnS_2 surface and (b) 1T-VS_2 surface. The direction of the arrow represents the migration path of one of the Li ions in Li_2S molecule as it breaks away from the molecule. The Li, S, Mn, and V atoms are marked as green, yellow, purple and red, respectively.

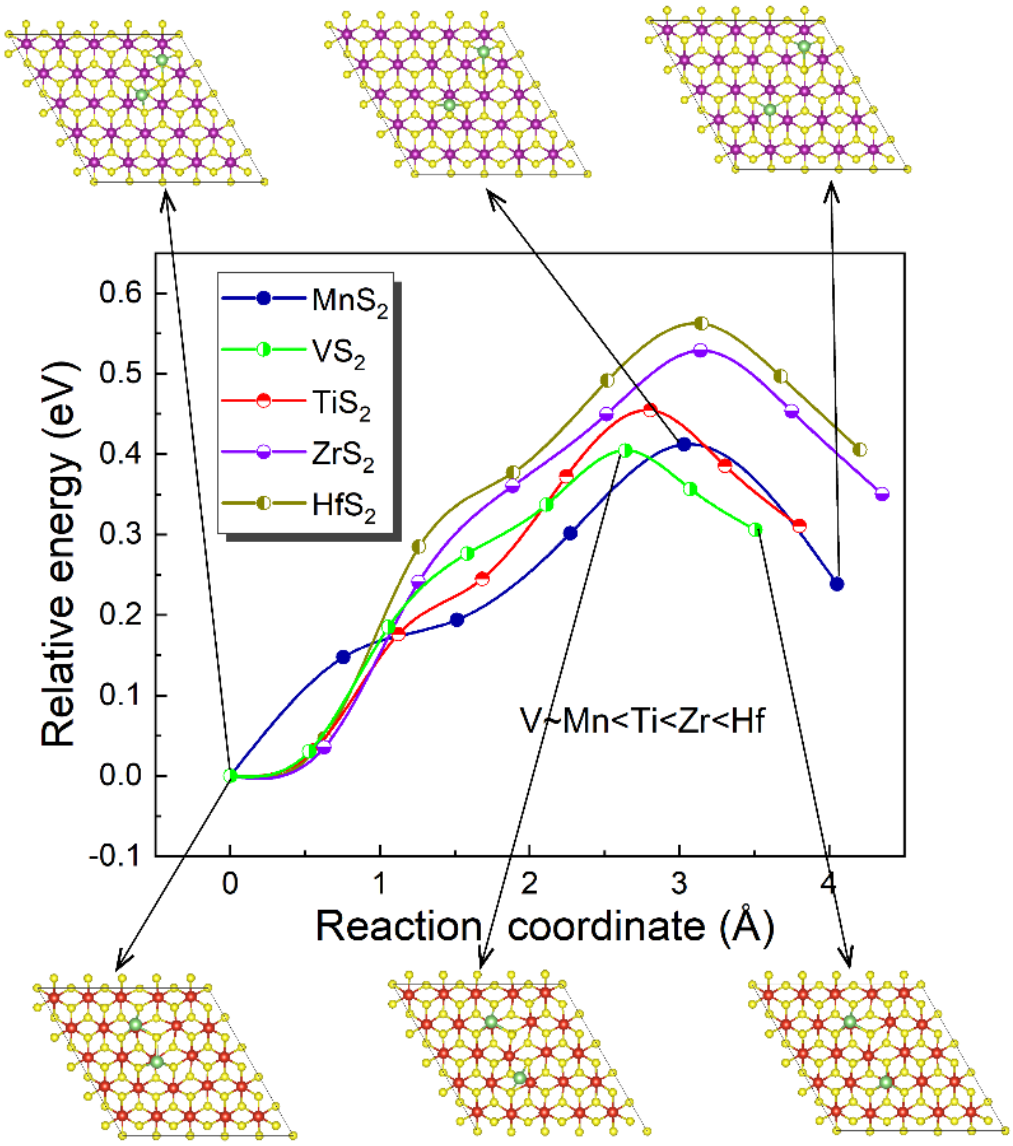

Fig. S9 The energy profile and atomic structure evolution for the decomposition of Li_2S

on 1T-MnS_2 and 1T-VS_2 surfaces. The Li, S, Mn, and V atoms are marked as green, yellow, purple and red, respectively. The three images in the top row demonstrate the evolution of the atomic structure of Li_2S decomposition on the surface of 1T-MnS_2, while the three images in the bottom row demonstrate the evolution of the atomic structure of Li_2S decomposition on the surface of 1T-VS_2.

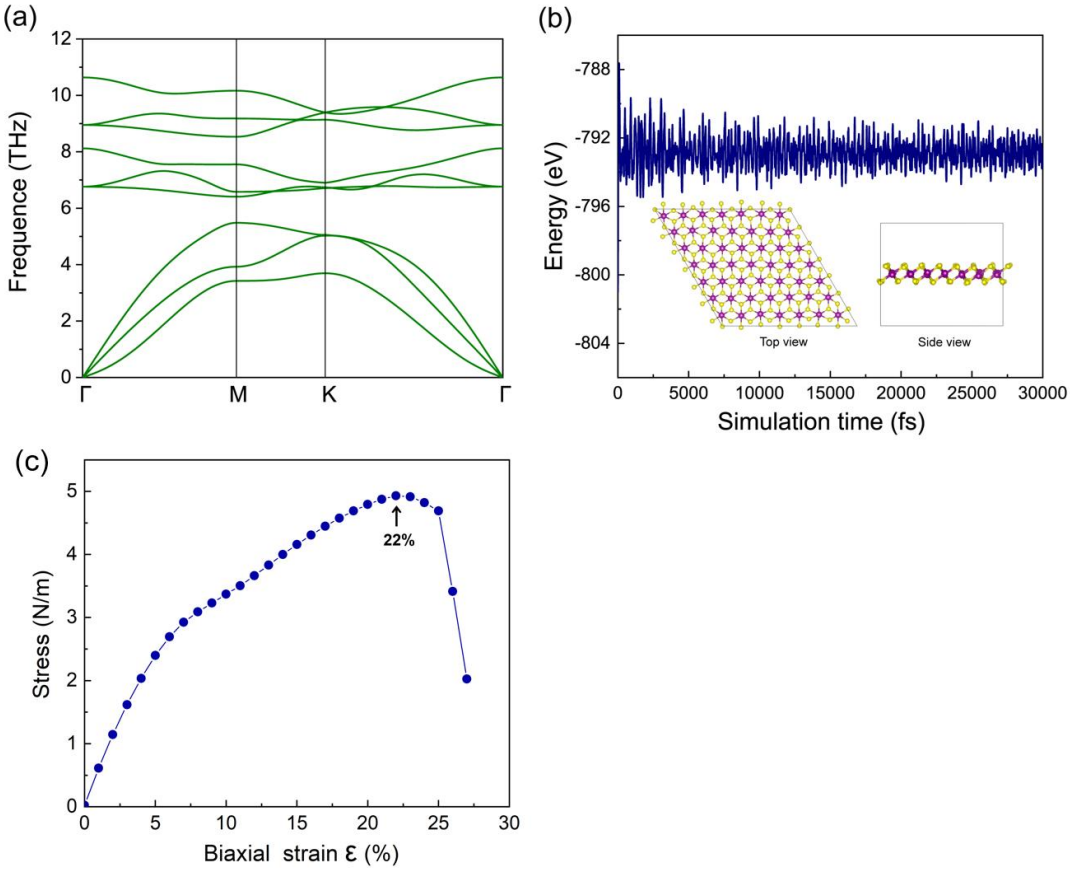

Fig. S10 The stability test for 1T-MnS_2. (a) The phonon dispersion curve, (b) AIMD simulation curve and (c) biaxial stress-strain response of 1T-MnS_2. Inset images are top and side views of 1T-MnS_2 after AIMD simulation of 30 ps at 400 K.

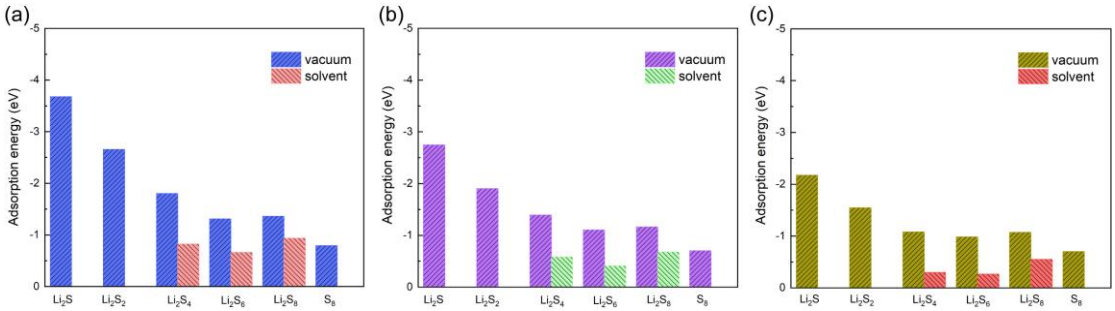

Fig. S11 The adsorption energy of Li_2S_n and S_8 on (a) 1T-VS_2, (b) 1T-ZrS_2 and (c) 1T-HfS_2 surfaces in vacuum and implicit solvent environment.

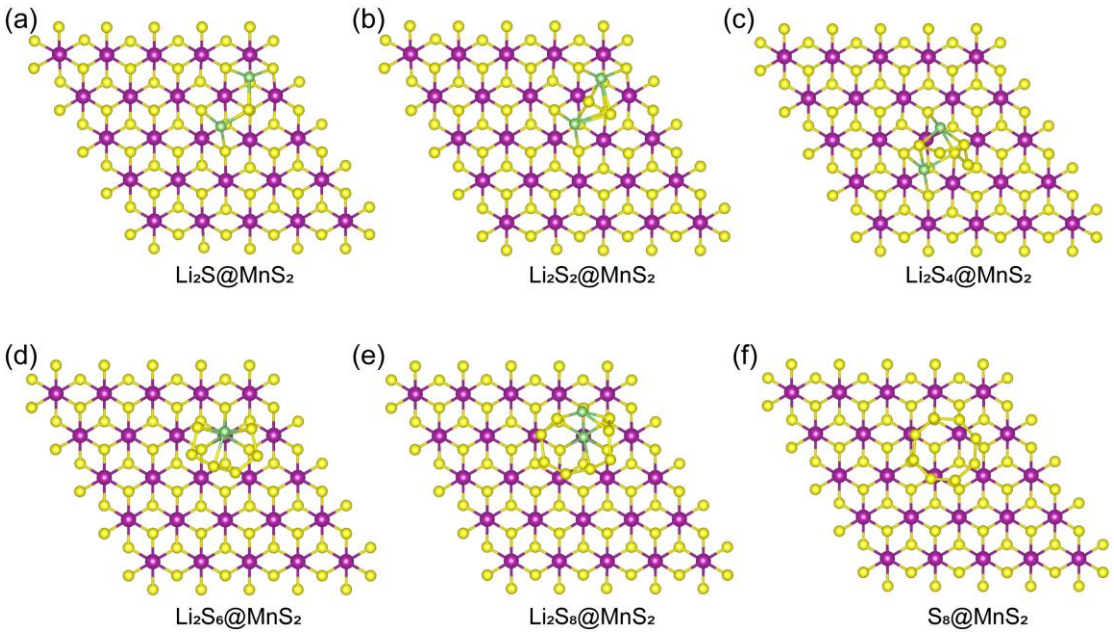

Fig. S12 The top views of adsorption configurations of Li_2S_n and S_8 on 1T-MnS_2 surface.

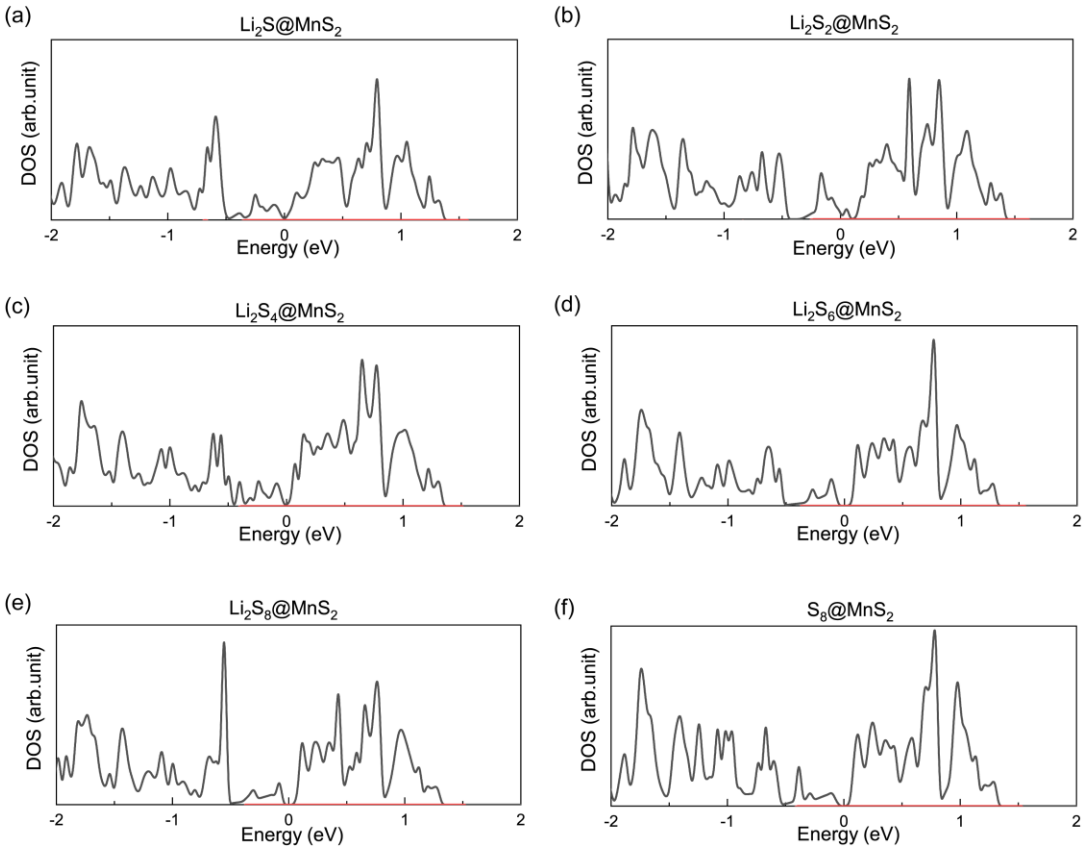

Fig. S13 Density of states for the adsorption configuration of Li_2S_n and S_8 on 1T-MnS_2 surface. Note that due to large energy gap in spin-down channel, only spin-up density of states is shown for the convenience of viewing energy gap influenced by adsorbed molecules. The Fermi level is set to 0 eV.

Table S1 The calculated bond length (*d*) and ICOHP of S-$S_{surface}$ bond on 1T-*M*S_2 surfaces when Li_2S molecule is adsorbed on 1T-*M*S_2 surfaces.

	MnS_2	VS_2	TiS_2	ZrS_2	HfS_2
d (Å)	2.03	2.07	2.05	2.07	2.15
ICOHP (eV)	-6.18	-5.58	-5.90	-5.61	-4.42

Table S2 Possible adsorption sites and the adsorption energy of Li ion on 1T-*M*S_2 surfaces. The bold part indicates the most likely site and the strongest adsorption among A, B, C sites for Li ion. NA represents A is local maximum site, and Li ion cannot be anchored to A site.

1T-*M*S_2	Adsorption energy of Li ion, $\boldsymbol{E_{ads}}$ **(eV)**		
	A	B	C
MnS_2	-2.93	-3.57	**-3.78**
VS_2	NA	**-3.39**	-3.33
TiS_2	NA	-3.65	**-3.68**
ZrS_2	NA	-3.17	**-3.27**
HfS_2	NA	-2.92	**-2.97**

Table S3 Possible diffusion modes and barriers of Li ion on 1T-*M*S_2 surfaces.

1T-*M*S_2	Possible diffusion modes					
	B-B	C-C	B-C	A-A	A-B	A-C
MnS_2	0.24	0.24	0.24	⩾0.24	⩾0.65	⩾0.85
VS_2	0.12	0.12	0.12	NA	NA	NA
TiS_2	0.17	0.17	0.17	NA	NA	NA
ZrS_2	0.18	0.18	0.18	NA	NA	NA
HfS_2	0.21	0.21	0.21	NA	NA	NA

Table S4 The calculated adsorption free energy (G_{ads}) of Li_2S_n and S_8 molecules, which was defined as $G_{\mathrm{ads}} = G_{\mathrm{total}} - G_{MS_2} - G_{\mathrm{molecule}}$. G_{MS_2}, G_{molecule} and G_{total} are the Gibb free energies of the 1T-MS$_2$ surface, the isolated molecule and the whole adsorbed system, respectively.

	MnS_2	VS_2	TiS_2	ZrS_2	HfS_2
$G_{\mathrm{ads}}(Li_2S)$	-3.92	-3.02	-3.14	-2.11	-1.56
$G_{\mathrm{ads}}(Li_2S_2)$	-2.91	-2.06	-2.07	-1.39	-1.05
$G_{\mathrm{ads}}(Li_2S_4)$	-1.94	-1.28	-1.49	-0.88	-0.56
$G_{\mathrm{ads}}(Li_2S_6)$	-0.67	-0.72	-0.78	-0.52	-0.41
$G_{\mathrm{ads}}(Li_2S_8)$	-0.61	-0.70	-0.82	-0.48	-0.38
$G_{\mathrm{ads}}(S_8)$	-0.07	-0.16	-0.16	-0.11	-0.07

Table S5 The calculated all ΔG when SRR occurs on the five 1T-MS$_2$ surfaces and in vacuum without catalyst.

	MnS_2	VS_2	TiS_2	ZrS_2	HfS_2	Vacuum
$\Delta G(S_8^* \rightarrow Li_2S_8^*)$	-3.18	-3.17	-3.29	-3.01	-2.95	-2.63
$\Delta G(Li_2S_8^* \rightarrow Li_2S_6^*)$	-0.12	-0.07	-0.02	-0.09	-0.08	-0.05
$\Delta G(Li_2S_6^* \rightarrow Li_2S_4^*)$	-0.98	-0.27	-0.42	-0.07	0.14	0.29
$\Delta G(Li_2S_4^* \rightarrow Li_2S_2^*)$	**-0.06**	**0.13**	**0.33**	**0.41**	**0.42**	**0.91**
$\Delta G(Li_2S_2^* \rightarrow Li_2S^*)$	-0.10	-0.05	-0.16	0.18	0.39	0.90

Table S6 The calculated energy gap (eV) of pristine 1T-MnS_2 and the total adsorbed system where sulfur species is on 1T-MnS_2 surface. The tag "*" represents the molecule absorbed on 1T-MnS_2 surface.

Spin channel	1T-MnS_2	Li_2S*	Li_2S_2*	Li_2S_4*	Li_2S_6*	Li_2S_8*	S_8*
Spin-up	0.10	0.00	0.00	0.00	0.10	0.09	0.06
Spin-down	1.97	1.94	1.91	1.97	1.97	1.94	1.97

Table S7 The calculated all ΔG when SRR occurs on four deformable 1T-MnS_2 surfaces.

	-4%-MnS_2	-2%-MnS_2	2%-MnS_2	4%-MnS_2
$\Delta G(S_8^* \rightarrow Li_2S_8^*)$	-3.15	-3.23	-3.27	-3.22
$\Delta G(Li_2S_8^* \rightarrow Li_2S_6^*)$	-0.16	-0.08	-0.03	0.00
$\Delta G(Li_2S_6^* \rightarrow Li_2S_4^*)$	-0.69	-0.83	-0.90	-1.14
$\Delta G(Li_2S_4^* \rightarrow Li_2S_2^*)$	**0.21**	**0.17**	**0.15**	**0.05**
$\Delta G(Li_2S_2^* \rightarrow Li_2S^*)$	0.03	0.03	-0.12	-0.09

Some discussion of Li-ion diffusion

According to the number of stable adsorption sites shown in Fig. 4(a) in the text and considering the reversibility of diffusion, there are 6 possible diffusion modes (A-A, B-B, C-C, A-B, A-C, B-C) for Li ion on MnS_2 surface, and there are 3 possible diffusion modes (B-B, C-C, B-C) for Li ion on VS_2, TiS_2, ZrS_2, HfS_2 surfaces, where the mode with the same initial and final sites is defined as the same mode. As shown in Fig. 4 in the text, a single Li ion diffusing on MnS_2, ZrS_2, HfS_2, and TiS_2 surfaces along C-B-C path (C-C mode) faces a barrier of 0.24 eV, 0.21 eV, 0.18 eV and 0.17 eV, while Li ion diffusing on VS_2 surface along B-C-B path (B-B mode) faces a barrier of 0.12 eV.

In the following, we will use the adsorption energy of Li on different sites and the energy barrier of our calculated diffusion path to argue that the diffusion barrier of other possible paths is not less in energy than the path in our calculation.

Take VS_2 surface as an example. We use CI-NEB method to calculate the diffusion barrier from a B site to its nearest B site and discovered that the lowest energy path is B-C-B with a barrier of 0.12 eV. Other possible paths, i.e. C-C and B-C, is equivalent to or is a subset of the B-C-B path, and therefore they should have the same energy barrier of 0.12 eV. Similar argument can be applied to TiS_2, ZrS_2 and HfS_2 surfaces.

For MnS_2 surface, we use CI-NEB method to calculate the diffusion barrier from a C site to its nearest C site and discovered that the lowest energy path is C-B-C with a barrier of 0.24 eV. Therefore, the diffusion paths B-C and B-C-B share the same energy barrier of 0.24 eV. **It is worth emphasizing that the energy barrier will be no less than the absolute value of the energy difference (that is, the adsorption energy difference) at the two nearest local stable sites of the diffusion path**. When Li-ion diffusion is along A-C or A-B mode, the absolute value of the adsorption energy difference between the initial and final sites is 0.85 eV or 0.65 eV (Table S2), which is higher than the energy barrier (0.24 eV) along C-B-C path. Similarly, when Li-ion diffusion is along A-A or B-B mode, Li ion may pass through C site due to strong adsorption of Li ion at C site, making the diffusion A-C-A or B-C-B path due to the strong adsorption at C site, hence the energy barrier cannot be no less than 0.24 eV. Therefore, a single Li ion diffusing on MnS_2 surfaces faces a minimum barrier of 0.24

eV.

In conclusion, a single Li ion diffusing on MnS_2, ZrS_2, HfS_2, TiS_2, and VS_2 surfaces faces a minimum barrier of 0.24 eV, 0.21 eV, 0.18 eV, 0.17 eV, and 0.12 eV, respectively. In addition, Li-ion diffusion can be along B-C-B-C-B-C-… or C-B-C-B-C-B-… path. Possible diffusion modes and barriers of Li ion on 1T-MS_2 surfaces are summarized in Table S3.